Marine Micropaleontology 71 (2009) 166–175

Contents lists available at ScienceDirect

Marine Micropaleontology

journal homepage: www.elsevier.com/locate/marmicro

The warm interglacial Marine Isotope Stage 31: Evidences from the calcareous nannofossil assemblages at Site 1090 (Southern Ocean)

Patrizia Maiorano [a,*], Maria Marino [a], José-Abel Flores [b]

[a] Dipartimento di Geologia e Geofisica, Università di Bari, Via E. Orabona, 4-70125 Bari, Italy
[b] Departamento de Geología, Facultad de Ciencias, Universidad de Salamanca, 37008 Salamanca, Spain

ARTICLE INFO

Article history:
Received 16 June 2008
Received in revised form 24 February 2009
Accepted 2 March 2009

Keywords:
Southern Ocean
ODP Site 1090
Mid-Pleistocene
Coccolithophores
Paleoceanography

ABSTRACT

Calcareous nannofossil assemblages have been investigated at Ocean Drilling Program (ODP) Site 1090 located in the modern Subantarctic Zone, through the Pleistocene Marine Isotope Stages (MIS) 34–29, between 1150 and 1000 ka. A previously developed age model and new biostratigraphic constraints provide a reliable chronological framework for the studied section and allow correlation with other records. Two relevant biostratigraphic events have been identified: the First Common Occurrence of *Reticulofenestra asanoi*, distinctly correlated to MIS 31–32; the re-entry of medium *Gephyrocapsa* at MIS 29, unexpectedly similar to what was observed at low latitude sites.

The composition of the calcareous nannofossil assemblage permits identification of three intervals (I–III). Intervals I and III, correlated to MIS 34–32 and MIS 30–29 respectively, are identified as characteristic of water masses located south of the Subtropical Front and reflecting the southern border of Subantarctic Zone, at the transition with the Polar Front Zone. This evidence is consistent with the hypothesis of a northward shift of the frontal system in the early Pleistocene with respect to the present position and therefore a northernmost location of the Subantarctic Front. During interval II, which is correlated to MIS 31, calcareous nannofossil assemblages display the most significant change, characterized by a distinct increase of *Syracosphaera* spp. and *Helicosphaera carteri*, lasting about 20 ky. An integrated analysis of calcareous nannofossil abundances and few mineralogical proxies suggests that during interval II, Site 1090 experienced the influence of subtropical waters, possibly related to a southward migration of the Subtropical Front, coupled with an expansion of the warmer Agulhas Current at the core location. This pronounced warming event is associated to a minimum in the austral summer insolation. The present results provide a broader framework on the Mid-Pleistocene dynamic of the ocean frontal system in the Atlantic sector of the Southern Ocean, as well as additional evidence on the variability of the Indian–Atlantic ocean exchange.

1. Introduction

The present study focuses on the response of the Pleistocene calcareous nannofossil assemblages in the interval between Marine Isotope Stage (MIS) 29 and MIS 34, at ODP Site 1090 (Gersonde et al., 1999), located in the eastern subantarctic sector of the Southern Ocean (Fig. 1). The investigated interval is of great interest since it includes MIS 31, which was the last significant warm interglacial of the obliquity-dominated climate regime and which may represent a precursor to the high-amplitude eccentricity-dominated cycles that followed the Mid-Pleistocene climate shift (Scherer et al., 2003; Scherer et al., 2008). The MIS 31 was recognized as a very warm interglacial interval by Froelich et al. (1991), but it has received very little attention so far. A southward migration of the Polar Front Zone (PFZ) has been inferred in this interval by Froelich et al. (1991) and Westall and Fenner (1991) at the South Atlantic Site 704 (Fig. 1). This hypothesis was based on the distribution of biosiliceous–calcareous composition of sediments, which represents a valuable tracer of the PFZ. More recently, new data collected in the Southern Ocean area, from nearshore deposits located in the McMurdo Sound, Antarctica (Scherer et al., 2003) and from deep-sea sediments recovered at ODP sites 1094 and 1165 (Teitler et al., 2007; Flores and Sierro, 2007; Villa et al., 2008; Scherer et al., 2008) (Fig. 1), pointed out that MIS 31 was a key climate event, which may have compromised the stability of the Antarctic Ice Sheet and produced a southward displacement of the Polar Front in the South Atlantic sector. All the mentioned data on the marine record come from the Antarctic and Polar Front Zones. Site 1090 is located in a northernmost position (42°54.8′S, 8°55.2′E) (Fig. 1), south of the modern Subtropical Front, in the area where the heat exchange between the Indian and South Atlantic oceans occurs (Lutjeharms, 1981, 1996). This region plays a crucial role on the global ocean circulation and on the Earth's climate system.

In order to reconstruct sea surface water dynamics during the Mid-Pleistocene, the composition of calcareous nannofossil assemblages

* Corresponding author. Tel.: +39 80 5443455; fax: +39 80 5442625.
E-mail address: p.maiorano@geo.uniba.it (P. Maiorano).

0377-8398/$ – see front matter © 2009 Elsevier B.V. All rights reserved.
doi:10.1016/j.marmicro.2009.03.002

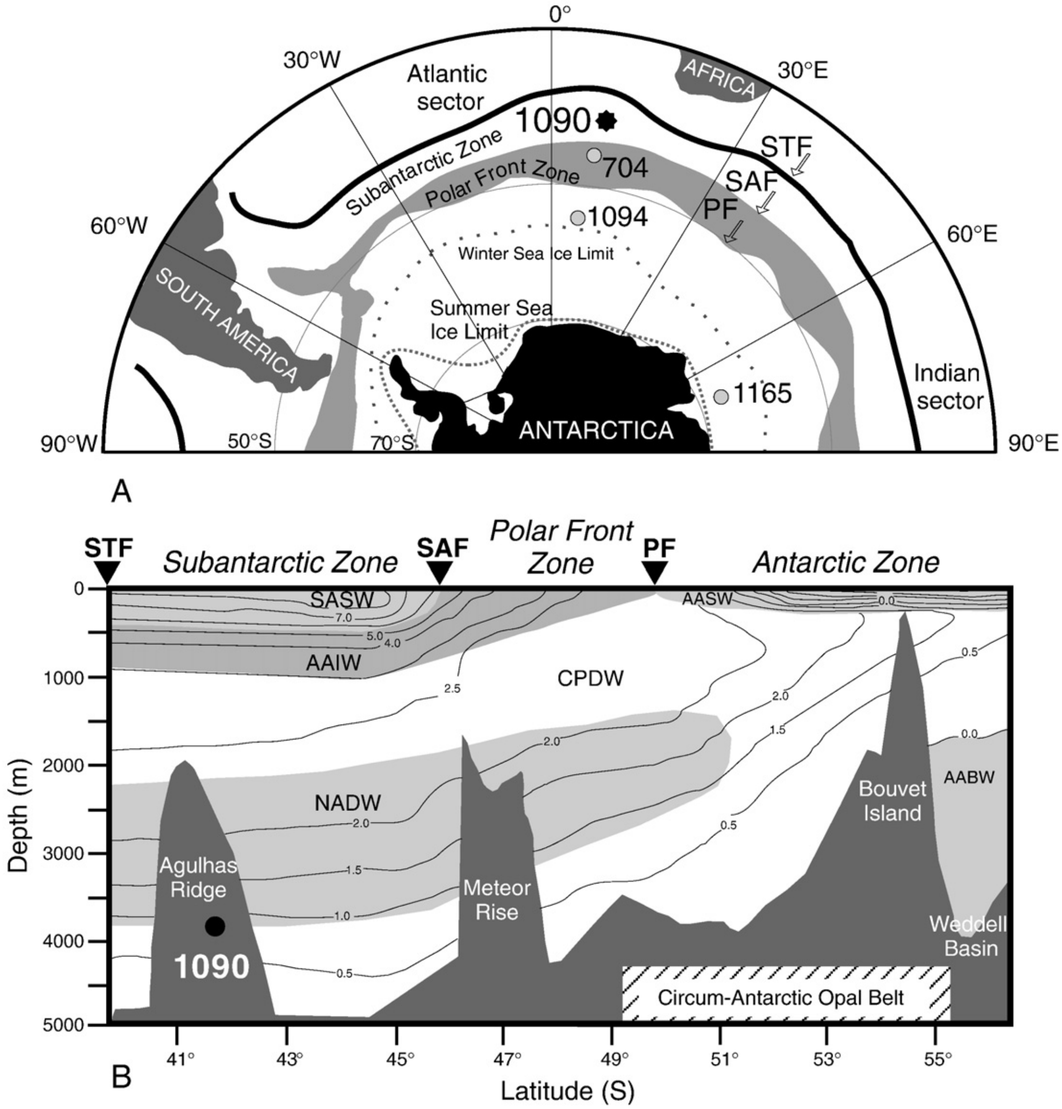

Fig. 1. A) Location of Site 1090 in the south-eastern Atlantic sector of the Southern Ocean, with the position of the modern oceanographic fronts and sea ice edge (Gersonde et al., 1999, modified). Location of additional sites cited in the text is also shown. STF: Subtropical Front; SAF: Subantarctic Front: PF: Polar Front. B) Vertical distribution of water masses and temperature (°C) on a north–south transect across the frontal system in the south-eastern South Atlantic. Modified from Gersonde et al. (1999). STF: Subtropical Front; SAF: Subantarctic Front; PF: Polar Front; SASW: Subantarctic Surface Water; AASW: Antarctic Surface Water; AAIW: Antarctic Intermediate Water; NADW: North Atlantic Deep Water; CPDW: Circumpolar Deep Water; AABW: Antarctic Bottom Water.

has been investigated at ODP Site 1090. Coccolithophores represent the main group of marine phytoplankton and are widely distributed in the world oceans (Roth, 1994). The composition of their assemblages reflects the horizontal pattern of water masses and therefore they represent a valuable tool to describe the ecological characteristics and the latitudinal boundaries of an investigated area. Several studies document the present distribution of coccolithophores in the South Atlantic Ocean (Eynaud et al., 1999; Findlay and Giraudeau, 2000; Boeckel and Baumann, 2004; Boeckel and Baumann, 2008) and their use as valuable tool for paleoclimatic and paleoceanographic proxy in the Southern Ocean (Okada and Wells, 1997; Flores et al., 1999; Baumann et al., 1999; Giraudeau et al., 2000).

2. Oceanographic setting

The hydrography of the southeastern South Atlantic is strongly determined by the position and flow regime of different zones, separated by a number of fronts (Fig. 1). The latter are characterized by rapid changes in water properties which occur over a short distance. Site 1090 is located in the middle of the modern Subantarctic Zone (SAZ) which is limited by the Subtropical Front (STF) to the north and by the Subantarctic Front (SAF) to the south (Fig. 1). The STF represents the boundary between warm, salty subtropical surface water and cooler, fresher Subantarctic Surface Water (Deacon, 1937). This front, in the eastern part of the Southern Atlantic, is located at around 40°S (Fig. 1A) and represents the most prominent surface thermal front, with a surface range in temperature and salinity of 17.9–10.6 °C and 35.5–34.3‰ respectively (Belkin and Gordon, 1996). Conversely, the SAF lies at about 46°S and marks the northern boundary of the Polar Front Zone, which is a transitional zone between Subantarctic Surface Water (SASW) and Antarctic Surface Water (AASW) (Fig. 1B); mean temperature and salinity surface values drop from 10.3 to 6.8 °C and 34.36 to 33.88‰ respectively (Belkin and Gordon, 1996).

Site 1090 is located on the southern flank of the Agulhas Ridge (Fig. 1B), at a water depth of 3699 m, near the present-day boundary between North Atlantic Deep Water (NADW) above and Circumpolar Deep Water (CDW) below, and above the calcium-carbonate compensation depth (CCD). The present location of Site 1090 is influenced by the distal filaments and eddies of the Agulhas Current (AgC, Fig. 2). The latter, which carries warm and salty water into the Southern Ocean, originates in the Indian Ocean and flows poleward along the East African coast. After entering the South Atlantic Ocean as highly energetic eddies or as small meandering filament waters, most of the current retroflects (Fig. 2) and returns to the Indian Ocean (Agulhas Return Current, AgR) (Lutjeharms, 1981, 1996). The southern boundary of the Agulhas Current system is represented by the Subtropical Convergence (Lutjeharms and Valentine, 1984). The frontal system formed by the Subtropical Convergence Zone and the Agulhas Return Current represents an area of elevated productivity (Cortese et al., 2004).

The transfer of heat and salt from Indian Ocean into the South Atlantic through the Agulhas Current is significant for regional weather and climate patterns (Lutjeharms, 1996; Reason 2001) and plays a key role in the global thermohaline circulation as well (Gordon, 1996). In fact, Agulhas rings, eddies and filaments form the source of the warm upper-layer water that flows northward through the Atlantic, in compensation for the colder southward flowing North Atlantic Deep Water (Gordon et al., 1992; Lutjeharms, 1996). The heat transfer by warm surface water trapped within the Agulhas Current to the atmosphere is believed to be the largest inter-ocean exchange in the Southern Hemisphere. This exchange is strongly related to the wind field over the South-Indian Ocean and to local dynamical processes around South Africa and is known to be variable on a seasonal scale (Lutjeharms, 1996; De Ruijter et al., 1999). The Agulhas water influx in the South Atlantic is favoured by a southward position of the STF (De Ruijter, 1982; Berger and Wefer, 1996). Further, the AgR is sensitive to the volume transport of the AgC (Lutjeharms and van Ballegooyen, 1984; Ou and de Ruijter, 1986). During austral summer, a westward penetration of the AgC into the South Atlantic Ocean, associated to a reduced retroflection is enabled by the southward migrated STF coupled with the reduced volume transport of the AgC. Few late Quaternary proxy records obtained from cores located close to the southern tip of Africa (Flores et al., 1999; Peeters et al., 2004) revealed that the magnitude of Indian–Atlantic water exchange is modulated on an orbital scale. These records also suggest a well-defined glacial–interglacial cyclicity, with a reduction of Agulhas leakage during glacial, in response to the increased sea ice cover and a northward position of the Subtropical Convergence and frontal zones.

3. Methods

3.1. Calcareous nannofossil analyses

The investigated sediments consist mainly of calcareous ooze (Gersonde et al., 1999). At Site 1090 calcareous nannofossil analyses have been performed in the interval from Cores 177-1090D-4H-5 through 4H-3. Samples were collected at about 2–5 cm, corresponding approximately to a temporal resolution of one sample per 1 kyr. Smear slides were prepared from unprocessed samples using standard methodologies (Bown and Young, 1998) and analysed under a polarized light microscope at 1000× magnification. Recent data on the reproducibility and accuracy of calcareous nannofossils assemblage counts (Blaj and Henderiks, 2007) conclude that smear slides are suitable for generating paleoecological data.

Being the small placoliths (<4 µm in size) an enormous part of the assemblage through most of the investigated interval, quantitative data were firstly collected by counting about 300 total nannofossils >4 µm in size. Although most of the small placoliths (small gephyrocapsids and small reticulofenestrids) are actually <3 µm in size, the separation at 4 µm was fixed in order to have a reliable pattern of the medium *Gephyrocapsa* group (4–5.5 µm in size), which has a relevant stratigraphic meaning in the Mid-Pleistocene records (Rio et al., 1990). In addition, a separate counting on 300 specimens of the total nannofossil assemblages has been performed in order to evaluate abundance patterns of *Florisphaera profunda* as suggested by Matsuoka and Okada (1989) and Castradori (1993) and of the dominant placoliths <4 µm. The number of the nannofossils >4 µm in size has been also recalculated with respect to the total assemblage counts, in order to evaluate the reliability of separate counting methods.

Following Beaufort et al. (2001) and Flores et al. (2000a) the relation between small placoliths and *F. profunda* has been tentatively considered as a paleoproductivity proxy, although *F. profunda* is not abundant at the studied site. This proxy has been calculated according to the *N* index proposed by Flores et al. (2000a):

$$N = R/(R + F)$$

where *R* is % of small placoliths, and *F* is % of *F. profunda*. However, the reliability of the *N* index in this southern region needs to be tested in other sites.

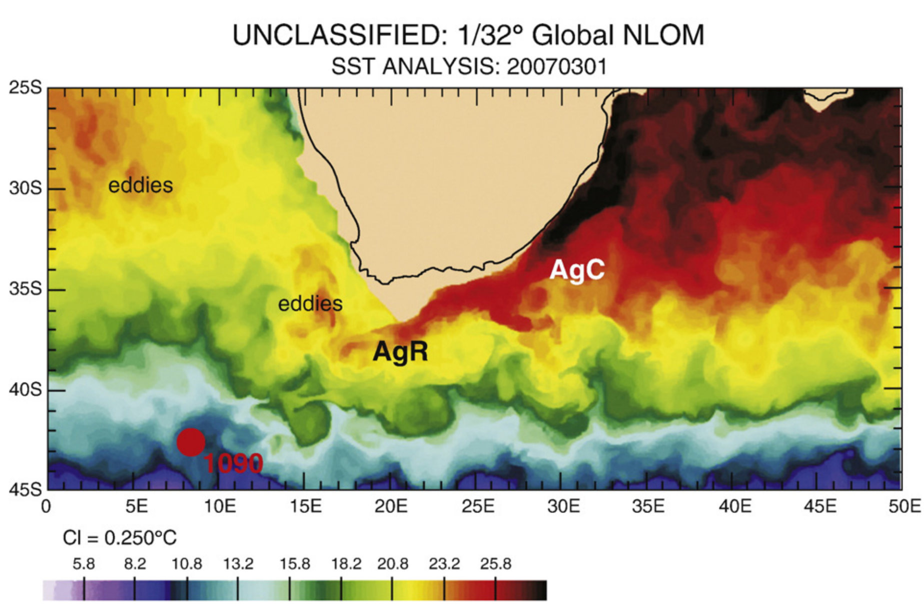

Fig. 2. Satellite image with the Sea Surface Temperature (SST) distribution in the Agulhas region on March 3rd, 2007. The image shows the expansion of the Agulhas Current in the South Atlantic during austral summer. From the online archive of the 1/32° Global Naval Layered Ocean Model (NLOM) real-time results of the Naval Research Laboratory, modified.

3.2. Principal Component Analyses

A multivariate statistical analyses using Principal Component Analysis (PCA) as extraction method was carried out in order to summarize the relationship between coccoliths distribution and few paleoenvironmental variables. The method allows to reduce a number of (possibly) correlated variables into a (smaller) number of uncorrelated variables called principal components. The software StatView 5.0.1 for Windows was used for this procedure. The involved data sets contain relative abundances of the most common taxa and few mineralogical variables. Within the calcareous nannofossil assemblage, the abundances of medium gephyrocapsids and *R. asanoi* have been omitted since their distribution is stratigraphically controlled. Taxa representing less than 2% of the assemblage (small *C. leptoporus*, *Oolithotus fragilis*, *Pontosphaera* spp., *Umbilicosphaera* spp., *Rhabdosphaera claviger*) have also been excluded. The mineralogical variables from the same samples (Diekmann and Kuhn, 2002), considered in the input matrix, include illite (Ill), kaolinite/chlorite (Kaol/Chl) ratio and quartz/feldspars (Qz/Fsp) ratio and are considered as proxies of regional ocean circulation (Petschick et al., 1996). The contribution of each variable and the explained variance are presented by means of an orthogonal plot where eigenvalues can be deduced from eigenvectors.

4. Results

4.1. Stratigraphy

Site 1090 is chronologically well constrained (Fig. 3) on the basis of $\delta^{18}O$ isotope stratigraphy (Venz and Hodell, 2002) and biostratigraphic data (Flores and Marino, 2002). The latter have been improved in the present study due to the increased sampling resolution (Fig. 3), thus refining the biostratigraphic framework of a key interval at southern mid-latitude settings. Specifically, the First Common Occurrence (FCO) of *R. asanoi* and the re-entry of medium *Gephyrocapsa* have been recorded. *R. asanoi* FCO is distinctly correlated to MIS 31–32 (Fig. 3), in good agreement with data from north Atlantic and Mediterranean sites (Maiorano and Marino, 2004). As discussed by Maiorano and Marino (2004), the different position of the First Occurrence (FO) of *R. asanoi* at MIS 35/34 (Wei, 1993; Flores et al., 2000b; Raffi, 2002) is probably related to different taxonomic criteria adopted by the different authors. The re-entry of medium *Gephyrocapsa* at Site 1090 is recorded close to MIS 29, matching the low latitude records. In fact, the event is known to occur at MIS 29 or 29/28 at low latitudes and at MIS 27–25 at high and mid-latitudes, both in the ocean sites and in the Mediterranean area (Raffi et al., 1993; Wei, 1993; Flores et al., 2000b; Raffi, 2002; Maiorano and Marino, 2004; Raffi et al., 2006). At present, the results from the mid-latitude setting of Site 1090 do not allow confirmation of the above mentioned event's diachrony.

4.2. Calcareous nannofossil assemblages

Calcareous nannofossils are common through the whole studied section. Biosiliceous fraction is always rare in the smear slides. Nannofossils are in a moderate-good state of preservation and no significant evidence of dissolution is recorded in the studied interval.

With regard to the total nannofossil assemblage (Fig. 4), it is evident that small placoliths are the dominant component, generally representing about 60–80% and even reaching 90% of the assemblage. Besides the small placoliths, the observed calcareous nannofossil assemblages through most of the studied interval (Fig. 4), appear characterized by *Coccolithus pelagicus* (mostly *C. pelagicus* ssp. *pelagicus*), *Calcidiscus leptoporus*, mostly represented by the morphotypes of 5–8 μm in size (intermediate type), and subordinately by morphotypes >8 μm in size (larger type) and <5 μm in size (smaller type). *Reticulofenestra* spp. (*R. asanoi*, *Reticulofenestra* sp. *sensu* Maiorano and Marino, 2004, and *R. minutula*) and *Pseudoemiliania lacunosa* have abundances between 20 and 30% (Fig. 4). Rare components are *Helicosphaera* spp. (mostly *H. carteri*), which constitute nearly 1–2% of the assemblage, although they have an increase during MIS 31, reaching abundances up to 4%

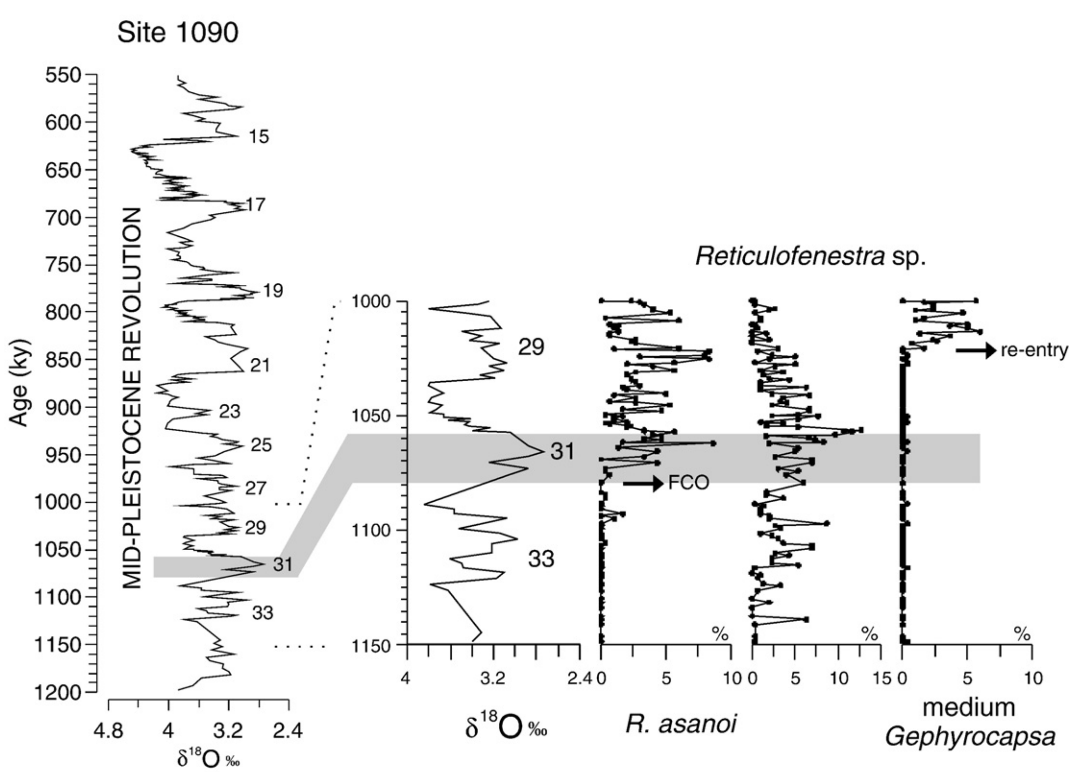

Fig. 3. Abundances of biostratigraphic markers at Site 1090 in the studied interval correlated to isotope chronology of Venz and Hodell (2002).

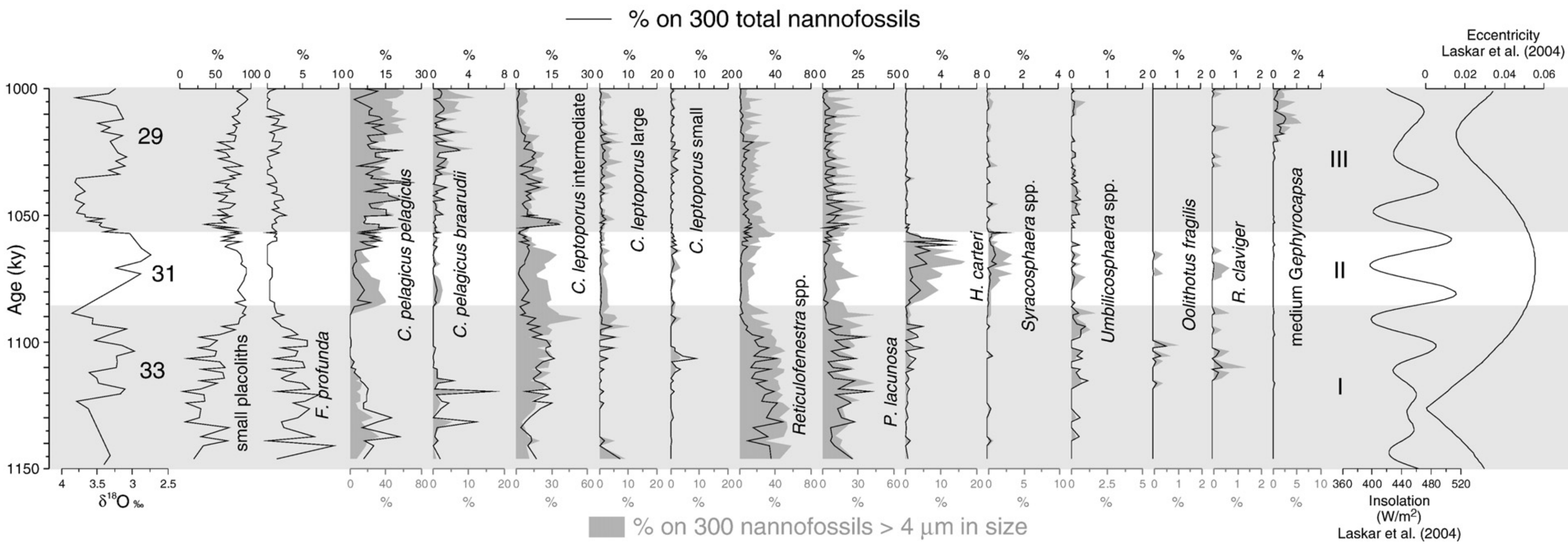

Fig. 4. Abundance patterns of calcareous nannofossils through the studied record. Intervals I–III are traced as discussed in the text. The abundance patterns of all the taxa are presented as % on 300 total nannofossils (black line) and as % on 300 nannofossils >4 µm in size (grey area). The correlation with the isotope chronology of Venz and Hodell (2002) and with the insolation target curve at 42°S (January–February) and of eccentricity of Laskar et al. (2004) is also shown.

(Fig. 4), and *Syracosphaera* spp. (mainly *Syracosphaera histrica*). *Syracosphaera* spp. are generally very rare (<1%) and shows a trend similar to *H. carteri*, being more frequent through MIS 31 (Fig. 4). *F. profunda* is a subordinate component as well and generally represents 1–4% of the assemblage (Fig. 4). Very rare taxa are *Umbilicosphaera* spp., *O. fragilis*, *R. claviger*, that totally represent less than 1% of the assemblage and are only sporadically encountered. The occurrence of medium *Gephyrocapsa* is stratigraphically restricted to the uppermost part of the studied interval (Fig. 4), in correspondence with MIS 29, where their reappearance bioevent indicates the small *Gephyrocapsa*–*P. lacunosa* zonal boundary of Rio et al. (1990). In this interval the taxon is never abundant and constitutes less than 2% of the assemblage (Fig. 4).

The results obtained from the different counting procedures (Fig. 4) indicate that the abundance patterns obtained from the counting on 300 total nannofossils match with those deriving from 300 nannofossils >4 µm. However, the counting on 300 nannofossils >4 µm, although providing an overestimation of the numerical abundances of taxa, highlights more distinctive trends. This is a consequence of the dominant small placoliths component, which prevented identification of a more representative number of those taxa >4 µm in size. In this context, based on the counting on 300 nannofossils >4 µm, the studied record can be differentiated in three intervals. Specifically, the first interval (I) corresponds to MIS 34 to 32 and is characterized by *Reticulofenestra* spp., *P. lacunosa*, *C. leptoporus* intermediate type and small placoliths. In addition, *F. profunda*, although never abundant, shows a consistent occurrence through interval I. The following interval (II) is coincident with MIS 31 and is discriminated by distinctive peaks in abundance of *H. carteri* and of *Syracosphaera* spp. This interval is characterized by a decrease in abundance of *Reticulofenestra* spp. and *F. profunda* and by an increase of small placoliths. An increase of *C. pelagicus* ssp. *pelagicus* and *C. pelagicus* ssp. *braarudii* is also observed. The third interval (III) corresponds to MIS 30–29 and is dominated by *C. pelagicus* ssp. *pelagicus* and small placoliths. In addition, *C. leptoporus* intermediate type and *P. lacunosa* are common components of the assemblage. *C. pelagicus* ssp. *braarudii*, although never abundant, is continuously present and shows a slight increase throughout this interval. Rare taxa such as *C. leptoporus* large type, *C. leptoporus* small type, *Umbilicosphaera* spp., *O. fragilis*, *R. claviger*, do not display any significant pattern through the three intervals. With regard to the *N* index (Fig. 5) it can be observed how it has a distinct increase from the upper part of interval I upwards.

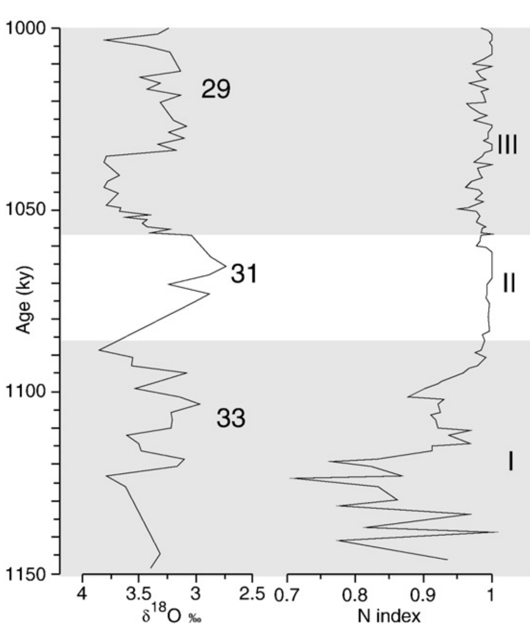

Fig. 5. Oxygen isotope record at Site 1090 and curve of *N* index.

5. Discussion

5.1. Paleoenvironmental interpretation

We have no evidence of a different state of preservation among samples belonging to different intervals. This feature suggests that the assemblages were not significantly modified by dissolution effect. Small placoliths' dominance is expected in the studied record, since it reflects a world-wide and well known Mid-Pleistocene paleoceanographic phenomenon (Gartner, 1977, 1988). With respect to the other important components of the assemblage, such as *C. pelagicus* and *C. leptoporus*, it can be remarked that these taxa are generally abundant at high-latitude late Quaternary records (Hiramatsu and De Deckker, 1997). Specifically, *C. pelagicus*, which is absent from the living community of the Southern Ocean (e.g. Findlay and Giraudeau, 2000), is considered a cold water indicator, ranging from 7–14 °C (McIntyre and Bé, 1967), or 0–10° (Baumann et al., 2000). On the other hand, temperature ranges of *C. leptoporus*, in the South Atlantic have been estimated at 5.4–14.2 °C (Findlay and Giraudeau, 2000). The taxon is abundant south of 40° (Hiramatsu and De Deckker, 1997) and becomes very rare south of the SAF (Eynaud et al., 1999). In more detail, the *C. leptoporus* intermediate type has been recorded as the most abundant of the three morphotypes, in all water-depths of the STFZ south of 40° (Boeckel and Baumann, 2008). It dominates over the larger morphotype, as at Site 1090, at low/intermediate water temperatures (Renaud et al., 2002). Considering the above mentioned biogeographic distributions and comparing the composition of the calcareous nannofossil assemblage with the ones recorded in the Southern Ocean (Hiramatsu and De Deckker, 1997; Flores et al., 1999; Findlay and Giraudeau, 2000; Boeckel et al., 2006), we infer that, with the exclusion of MIS 31, the common occurrence of *C. leptoporus* intermediate type and *C. pelagicus* ssp. *pelagicus* are in agreement with water masses located south of the STF. More specifically, the assemblages seem to reflect the southern border of SAZ at the transition with the Polar Front Zone as also suggested by the sporadic occurrences or absence of taxa such as *Syracosphaera* spp., *Rhabdosphaera* spp., *Umbilicosphaera* spp., *O. fragilis*, which are important component of the Subantarctic Zone and very rare or absent in the Polar Front Zone (Eynaud et al., 1999). This interpretation is in good agreement with the assessment of a long-term northward shift of the frontal system in the early Pleistocene (1.83–0.87 Ma) with respect to the present (Becquey and Gersonde, 2002), based on the planktonic foraminifera Sea Surface Temperature record at Site 1090.

According to the calcareous nannofossil abundance patterns, short-term modifications in the sea surface water conditions seem to have occurred through the studied record. In order to better clarify the complex relationship between coccolithophorids and paleoenvironmental conditions occurring through intervals I–III, a multivariate statistical analyses by means of Principal Component Analysis (PCA) method has been performed (Fig. 6). The abundance of the most common calcareous nannofossil taxa together with illite (Ill) content, kaolinite/chlorite (Kaol/Chl) and quartz/feldspars (Qz/Fsp) ratios from the same samples (Diekmann and Kuhn, 2002) have been considered as variables in the input matrix. These mineralogical variables are considered significant tracers of latitudinal shifts in watermass boundaries (Diekmann et al., 1996; Diekmann and Kuhn, 2002; Diekmann et al., 2003). Specifically, illite represents the major proximal input of clay mineral from southern Africa, while kaolinite and chlorite indicate a more distal input and characterize a small proportion of the clay-mineral assemblage (Petschick et al., 1996). The kaolinite and chlorite content dilutes the dominant terrigenous input of illite-rich material from southern Africa (Diekmann and Kuhn, 2002). Kaolinite mainly originates in deeply weathered soils and rocks of tropical and subtropical Africa and is delivered through fluvial discharge to both the South Atlantic and the Indian Ocean (Diekmann et al., 2003 and references therein). On the other hand, chlorite

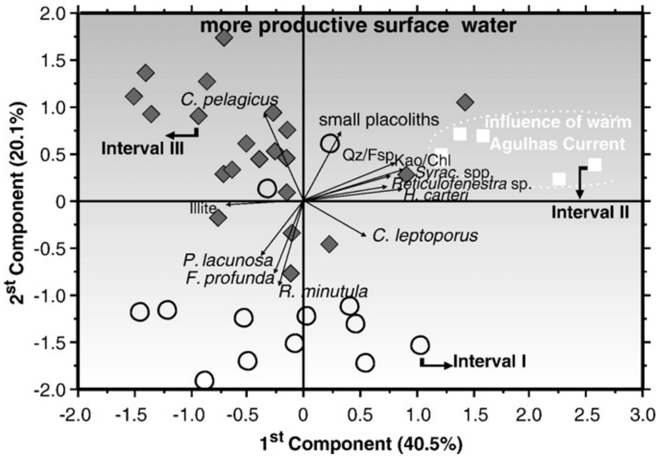

Fig. 6. Orthogonal plot of the multivariate statistical analysis carried out using Principal Component Analysis (PCA) as extraction method. In the input matrix both calcareous nannofossil abundances and mineralogical variables of Diekmann and Kuhn (2002) have been used.

represents a typical high-latitude clay mineral, that characterizes the detrital particulate load of Circum Polar Deep Water (CPDW). Cyclic fluctuations of Kao/Chl and Qz/Fsp ratios, with high values during interglacial periods, follow the southward propagation of kaolinite and quartz-rich suspensions entrained in the filaments of the Agulhas Current and within NADW (Petschick et al., 1996; Kuhn and Diekmann, 2002; Diekmann et al., 2003).

The results of the PCA (Fig. 6) indicate that the first component (40% of total variance) groups together Kaol/Chl and Qz/Fsp ratios, *H. carteri*, *Syracosphaera* spp. and *Reticulofenestra* sp. with high positive component loadings, and Ill content with a negative component loading. *C. leptoporus* (intermediate and large types) displays a low factor score (−0.495) due to its rather uniform pattern through the whole interval. In the 1st component vs. 2nd component plot (Fig. 6), samples from interval II (MIS 31), are distinctly separated from those of intervals I and III and fall in the direction of maximum variation of Kaol/Chl and Qz/Fsp ratios. Based on the relation between clay-mineral assemblage and characteristics of water masses in the studied area, the first component seems to reflect the influx of the warmer Agulhas Current eddies at the core location, which increases during interval II, as well as a far southward injection of NADW. The relation of *H. carteri* and *Syracosphaera* spp. with Kaol/Chl and Qz/Fsp ratios and their increase during interval II is also interesting and supports the interpretation mentioned above. *Syracosphaera* spp., are considered as warm and oligotrophic taxa (McIntyre et al., 1972; Roth and Coulbourn, 1982; Pujos, 1992; Haidar and Thierstein, 1997; Jordan et al., 1996; Flores et al., 1999; Findlay and Giraudeau, 2000; Baumann et al., 2004; Ziveri et al., 2004). *H. carteri* is known to have affinities for warm waters (McIntyre and Bé, 1967, Gard and Backman, 1990; Brand, 1994) and moderately elevated nutrient conditions (Ziveri et al., 1995; Ziveri et al., 2000; Andruleit and Rogalla, 2002; Findlay and Giraudeau, 2002; Ziveri et al., 2004). High abundance of *H. carteri* is recorded during high productivity episodes (Pujos, 1992; Flores et al., 1995) and in upwelling regions (Estrada, 1978; Giraudeau, 1992). Ziveri et al. (2004) clearly show that *H. carteri* is mainly occurring in the mesotrophic equatorial divergence belt. Positive relations between abundances of *Helicosphaera* spp. and *Syracosphaera* spp. with lower salinity and terrigenous input of surface water have been also inferred (Weaver and Pujol, 1988; Flores et al., 1997; Colmenero-Hidalgo et al., 2004; Flores and Sierro, 2007). In spite of their complex paleoecological requirements, it seems significant that in the Southern Ocean these taxa have been associated to warmer intervals (Gard, 1989; Wells and Okada, 1997; Hiramatsu and De Deckker, 1997, Findlay and Flores, 2000). Furtherly, it is worthy to note that Flores et al. (1999) observed an increase in the abundance of *H. carteri* and *Syracosphaera* spp. in the surface sediment calcareous nannofossil assemblages of the Subtropical Convergence/Agulhas Current domain, with respect to the ones of the Subantarctic Zone. It is therefore reasonable to assume that during interval II, the strong positive relation between *H. carteri* and *Syracosphaera* spp. with Kaol/Chl and Qz/Fsp reflects the influence, at Site 1090, of the warmer Agulhas Current and a related southward migration of the STF, which probably reached the core location. These data are consistent with a distinct Sea Surface Temperature increase at MIS 31 as recorded by Becquey and Gersonde (2002) at the same site. However the presence of garnet clasts recorded during MIS 31 at Site 1090 (Teitler et al., 2007), and interpreted as a provenance of the rafting iceberg from East Antarctica may suggest that the increase of *H. carteri* and *Syracosphaera* spp. is also the result of reduced salinity related to Antarctica ice melting (Flores and Sierro, 2007; Scherer et al., 2008).

The second component (20% of total variance) groups together *C. pelagicus* and small placoliths with positive component loadings and *F. profunda* and *R. minutula* with negative component loadings. A rather low factor score (0.495) is recorded for *P. lacunosa* as also observed above for *C. leptoporus* for the 1st component. *R. minutula* does not help to improve the accuracy of the paleoenvironmental interpretation since the ecological requirements of the taxon are poorly known. In the 1st component vs. 2nd component plot (Fig. 6) samples of interval I fall in the maximum direction of *F. profunda*, while samples of intervals II and III display an increase in *C. pelagicus* and of small placoliths. In our record (Fig. 4) *C. pelagicus* is mostly represented by the cold sub-Arctic *C. pelagicus* ssp. *pelagicus* and, secondarily, by the temperate *C. pelagicus* ssp. *braarudii* which is related to upwelling conditions (Baumann, 1995; Baumann et al., 2000; Cachao and Moita, 2000; Parente et al., 2004; Narciso et al., 2006). However, both the taxa have comparable distribution through time (Fig. 4). Small placoliths, which are essentially represented by small *Gephyrocapsa* and small reticulofenestrids, are considered opportunistic taxa of the upper photic zone (Gartner et al., 1987; Gartner, 1988; Okada and Wells, 1997), which bloom in surface waters of upwelling areas (Gartner, 1988; Okada and Wells, 1997; Takahashi and Okada, 2000) and indicate eutrophic condition (Gartner et al., 1987; Gartner, 1988; Takahashi and Okada, 2000; Colmenero-Hidalgo et al., 2004; Flores et al., 2005). On the other hand, the deep-photic zone taxon *F. profunda*, which thrives in well-stratified, low temperature, nutrient-rich waters, has been used as an indicator of the depth of the nutricline (Okada and Honjo, 1973; Molfino and McIntyre, 1990). Accordingly, higher values of the *N* index have been interpreted as an indication of higher productivity in the upper photic zone (Flores et al., 2000a; Colmenero-Hidalgo et al., 2004). Therefore, we suggest that the 2nd component may reflect productivity of surface waters, implying a more productive environment during intervals II and III with respect to interval I. The pattern of the *N* index, showing an increase during intervals II and III (Fig. 5), is in agreement with this interpretation. We infer that the increased productivity was a consequence of the southward frontal displacement. However, the composition of calcareous nannofossil assemblage indicates that the most prominent change occurred during interval II, in response to frontal displacement, influx of warm Aghulas Current and, possibly, to melting processes.

5.2. Paleoceanographic and paleoclimatic implication

The micropaleontological and mineralogical proxies across MIS 34–29 reveal that during MIS 31, a major climate modification affected Site 1090, leading to a southward migration of the STF and to an expansion of the influence of the Agulhas Current at the core location. This phenomenon appears as an amplified climate signal with respect to the normal obliquity-dominated glacial–interglacial cyclicity. The isotope chronology available at Site 1090 lets us compare the results with the insolation curve at 42°S (Laskar et al., 2004), as shown in Fig. 4. The interval II falls within an interval of high-amplitude insolation variability and of an eccentricity cycle and specifically is mainly centred to an insolation minimum. This result supports the hypothesis of a superimposed insolation forcing on the Agulhas Current variability (Peeters et al., 2004; Cortese et al., 2004) and is consistent with the idea that the lower austral summer insolation, together with deglacial warming of MIS 31 at higher latitudes, reduced both meridional temperature gradient and wind forcing as well as the volume transport of the AgC (Pether, 1994). These features may have favoured the westward protrusion of the AgC into the South Atlantic (Ou and de Ruijter, 1986). Our results match with data from core sites located in southern Cape Basin (Peeters et al., 2004), a location which is more sensitive to monitor the increase in the strengthening of the Agulhas leakage. Here, the inter-ocean exchange becomes stronger (increase in mass transport and sharper/earlier retroflection) at the end of each of the last five glacial periods. This pattern is possibly the response to increased strength of the monsoon system that promoted the equatorial transport of warm tropical waters feeding the Agulhas current (Schouten et al., 2002; Peeters et al., 2004). The most distal position of Site 1090 is more sensitive to document major westward protrusion of the AgC in the South Atlantic, rather than strengthening in the inter-ocean leakage. The paleoenvironmental modification recorded at Site 1090 during MIS 31 is well consistent with evidence of an extreme warming event from Antarctic nearshore deposits during MIS 31 (Scherer et al., 2003, 2008), which may have promoted a possible collapse of the Western Antarctic Ice Sheet, with the recognition of a warming event occurring at about 1 Ma in the East Antarctica (Teitler et al., 2007; Villa et al., 2008) and of a southward displacement of the Polar Front at ODP Site 704 (Froelich et al., 1991) and 1094 (Flores and Sierro, 2007). These evidence suggest that this distinct warm event is likely the result of a modification in the poleward heat transport and/or polar amplification of an orbital induced climate event, which may have affected both the stability of the Antarctic ice sheet and the global thermohaline circulation.

6. Conclusion

The quantitative analyses on calcareous nannofossil assemblage at ODP Site 1090 provide a refinement of the biostratigraphic constraints in the Southern Ocean and allow us to recognize significative paleoenvironmental modifications at the Mid-Pleistocene interval through MIS 34–29. Specifically, the FCO of *R. asanoi* is recorded at MIS 31–32 confirming its high correlation potential. It can be considered a reliable bioevent for the identification of this key interval on a global scale. The re-entry of medium *Gephyrocapsa* is associated to MIS 29, similarly to low latitude records; therefore, the well known diachrony of this event between the low and the mid-high latitude is not confirmed in the southern hemisphere, from the investigated mid-latitude record. The composition of the calcareous nannofossil assemblages at ODP Site 1090 suggests a northernmost location of the SAF during most of the studied interval as previously documented by Becquey and Gersonde (2002) at the same site. A distinct increase in the abundance of *H. carteri* and of *Syracosphaera* spp., lasting about 20 ky, within MIS 31, is interpreted as a response to a sea surface warming event and enhanced productivity, possibly accompanied by reduced salinity. Correlation with calcareous nannofossil assemblages known from the Subtropical Convergence/Agulhas Current domain and with few mineralogical proxies at the same site suggests that the recognized sea surface water change can be related to a major expansion of warm eddies and filaments of the Agulhas Current. This signal supports the hypothesis of an insolation forcing on the Agulhas Current variability, superimposed to the normal obliquity-dominated glacial–interglacial cyclicity.

The evidence of this anomalous warming event, previously identified from other Southern Ocean locations, is now highlighted by calcareous nannofossil assemblage at a more distal Site 1090, thus confirming that it was a distinct Mid-Pleistocene paleoclimatic event.

Acknowledgements

We wish to thank the Ocean Drilling Program for providing samples of the investigated site. We also acknowledge Bernard Diekmann who made available the mineralogical data set. The critical reviews of K.-H. Baumann and I. Raffi are greatly acknowledged. This research was financially supported by Fondi di Ateneo, Università di Bari, R. La Perna, 2006.

Appendix A. List of taxa cited in the text

Calcidiscus Kamptner, 1950
C. leptoporus (Murray and Blackman, 1898) Loeblich and Tappan, 1978
C. leptoporus small (<5 µm), intermediate (5–8 µm) and large (>8 µm) have been differentiated using the morphometric criterion, because other morphological characters are not detectable in LM analysis.
Coccolithus Schwarz, 1894
C. pelagicus (Wallich, 1877) Schiller, 1930 ssp. *pelagicus*
C. pelagicus ssp. *braarudii* (Gaarder, 1962) Geisen et al., 2002
Florisphaera Okada and Honjo 1973
Florisphaera profunda Okada and Honjo, 1973
Gephyrocapsa Kamptner, 1943
G. oceanica s.l >4 m *sensu* Rio, 1982
G. omega Bukry, 1973
Helicosphaera Kamptner, 1954
H. carteri (Wallich, 1877) Kamptner, 1954
H. hyalina (Gaarder, 1970) Jordan and Young, 1990
H. wallichi, Theodoridis, 1984
H. pavimentum (Okada and McIntyre, 1977)
Helicosphaera granulata (Bukry and Percival, 1971) Jafar and Martini, 1975
H. neogranulata (Gartner, 1977)
Oolithotus Reinhardt in Cohen and Reinhardt, 1968
O. fragilis (Lohmann, 1912) Martini and Müller, 1972
Pontosphaera Lohmann, 1902
Pseudoemiliania Gartner, 1969
P. lacunosa (Kamptner, 1963) Gartner, 1969
small placoliths include placoliths <4 µm in size
Reticulofenestra Hay et al., 1966
R. asanoi Sato and Takayama, 1992
R. minutula (Gartner, 1967) Haq and Berggren, 1978
Reticulofenestra sp. (*sensu* Maiorano and Marino, 2004)
Rhabdosphaera Haeckel, 1894
R. claviger Murray and Blackman, 1898
Syracosphaera Lohmann, 1902
S. histrica Kamptner, 1941
Umbilicosphaera Lohmann, 1902

Appendix B. Supplementary data

Supplementary data associated with this article can be found, in the online version, at doi:10.1016/j.marmicro.2009.03.002.

References

Andruleit, H.A., Rogalla, U., 2002. Coccolithophores in surface sediments of the Arabian Sea in relation to environmental gradients in Surface waters. Mar. Geol. 186, 505–526.
Baumann, K.-H., 1995. Morphometry of Quaternary *Coccolithus pelagicus* coccoliths from Northern Atlantic and its paleoceanographic significance. In: Flores, J.-A., Sierro, F.J. (Eds.), 5th INA Conference in Salamanca Proceedings, pp. 11–21.

Baumann, K.-H., Cepek, M., Kinkel, H., 1999. Coccolithophores as indicators of ocean water masses, surface-water temperature, and paleoproductivity examples from the South Atlantic. In: Fischer, G., Wefer, G. (Eds.), Use of Proxies in Paleoceanography: Examples from the South Atlantic. Springer, Berlin, pp. 117–144.
Baumann, K.-H., Andruleit, H., Samtleben, C., 2000. Coccolithiphores in the Nordic Seas: comparison of living communities with surface sediment assemblages. Deep-Sea Res. II 47, 1743–1772.
Baumann, K.-H., Bockel, B., Frenz, M., 2004. Coccolith contribution in the South Atlantic carbonate sedimentation. In: Thierstein, H.R., Young, J.R. (Eds.), Coccolithophores — From Molecular Processes to the Global Impact. Springer, Berlin, pp. 367–402.
Beaufort, L., de Garidel-Thoron, T., Mix, A.C., Pisias, N.G., 2001. ENSO-like forcing on oceanic primary production during the late Pleistocene. Science 293, 2440–2444.
Becquey, S., Gersonde, R., 2002. Past hydrographic and climatic changes in the Subantarctic Zone — the Pleistocene record from ODP Site 1090. Palaeogeogr. Palaeoclimatol. Palaeoecol. 182, 221–239.
Belkin, I.M., Gordon, A.L., 1996. Southern Ocean fronts from the Greenwich meridian to Tasmania. J. Geophys. Res. 101, 3675–3696.
Berger, W.H., Wefer, G., 1996. Expeditions into the past: paleoceanographic studies in the South Atlantic. In: Wefer, G., Berger, W.H., Siedler, G., Webb, D.J. (Eds.), The South Atlantic: Past and Present Circulation. Springer-Verlag, Berlin, pp. 363–410.
Blaj, T., Henderiks, J., 2007. Smear and spray preparation techniques put to the test (II): reproducibility and accuracy of calcareous nannofossil assemblage counts. J. Nannoplankton Res. 29 (2), 92–100.
Boeckel, B., Baumann, K.-H., 2004. Distribution of coccoliths in surface sediments of south-eastern South Atlantic Ocean: ecology, preservation and carbonate contribution. Mar. Micropaleontol. 51, 301–320.
Boeckel, B., Baumann, K.-H., 2008. Vertical and lateral variations in coccolithophore community structure across the subtropical frontal zone in the South Atlantic Ocean. Mar. Micropaleontol. 67, 255–273.
Boeckel, B., Baumann, K.-H., Henrich, R., Kinkel, H., 2006. Coccolith distribution patterns in South Atlantic and Southern Ocean surface sediments in relation to environmental gradients. Deep-Sea Res. I 53, 1073–1099.
Bown, P.R., Young, J.R., 1998. Chapter 2: techniques. In: Bown, P.R. (Ed.), Calcareous Nannofossil Biostratigraphy. Kluwer Academic Publishing, Dordresht, pp. 16–28.
Brand, L.E., 1994. Physiological ecology of marine coccolithophores. In: Winter, A., Siesser, W. (Eds.), Coccolithophores. Cambridge University Press, Cambridge, pp. 39–49.
Cachao, M., Moita, M.T., 2000. Coccolithus pelagicus, a productivity proxy related to moderate fronts off Western Iberia. Mar. Micropaleontol. 39, 131–155.
Castradori, D., 1993. Calcareous nannofossils and the origin of eastern Mediterranean sapropel. Paleoceanography 8 (4), 459–471.
Colmenero-Hidalgo, E., Flores, J.A., Sierro, J., Barcena, M.A., Lowemark, L., Schonfeld, J., Grimalt, J.O., 2004. Ocean surface water response to short-term climate changes revealed by coccolithophores from the Gulf of Cadiz (NE Atlantic) and Alboran Sea (W Mediterranean). Paleogeogr. Paleoclim. Paleoecol. 205, 317–336.
Cortese, G., Abelmann, A., Gersonde, R., 2004. A glacial warm water anomaly in the subantarctic Atlantic Ocean, near the Agulhas Retroflection. Earth Planet. Sci. Lett. 222, 767–778.
De Ruijter, W.P.M., 1982. Asymptotic analysis of the Agulhas and Brazil Current systems. J. Phys. Oceanogr. 12, 361–373.
De Ruijter, W.P.M., Biastoch, A., Drijfhout, S.S., Lutjeharms, J.R.E., Matano, R.P., Pichevin, T., van Leeuwen, P.J., Weijer, W., 1999. Indian–Atlantic interocean exchange: dynamics, estimation and impact. J. Geophys. Res. 104 (C9), 20855–20910.
Deacon, G.E.R., 1937. The hydrology of the southern ocean. Discov. Rep. 15, 3–122.
Diekmann, B., Kuhn, G., 2002. Sedimentary record of the mid-Pleistocene climate transition in the sub-Antarctic South Atlantic (ODP Site 1090). Palaeogeogr. Palaeoclimatol. Palaeoecol. 182, 241–258.
Diekmann, B., Petschick, R., Gingele, F.X., Fütterer, D.K., Abelmann, A., Brathauer, U., Gersonde, R., Mackensen, A., 1996. Clay mineral fluctuations in late Quaternary sediments of the southeastern South Atlantic: implications for past changes of deep water advection. In: Wefer, G., Berger, W.H., Siedler, G., Webb, D. (Eds.), The South Atlantic: Present and Past Circulation. Springer, Berlin, pp. 621–644.
Diekmann, B., Fälker, M., Kuhn, G., 2003. Environmental history of the south-eastern South Atlantic since the Middle Miocene: evidence from the sedimentological records of ODP Sites 1088 and 1092. Sedimentology 50, 511–529.
Estrada, M., 1978. Mesoscale heterogeneities of the phytoplankton distribution. In: Boje, R., Tomezak, M. (Eds.), The Upwelling Region of North West Africa. (Upwelling Ecosystems). Springer, Berlin, pp. 15–23.
Eynaud, F., Giraudeau, J., Pichon, J.J., Pudsey, C.J., 1999. Seasurface distribution of occolithophores, diatoms, silicoflagellates and dinoflagellates in the South Atlantic Ocean during the late austral summer 1995. Deep-Sea Res. I 46, 451–482.
Findlay, C.S., Flores, J.A., 2000. Subtropical Front fluctuations south of Australia (45°09′S, 146°17′E) for the last 130 ka years based on calcareous nannoplankton. Mar. Micropaleontol. 40, 403–416.
Findlay, C.S., Giraudeau, J., 2000. Extant calcareous nannoplankton in the Australia sector of the southern ocean (Austral summer 1994 and 1995). Mar. Micropaleontol. 40, 417–439.
Findlay, C.S., Giraudeau, J., 2002. Movement of oceanic fronts south Australia during the last 10 ka: interpretation of calcareous nannoplankton in surface sediments from the Southern Ocean. Mar. Micropaleontol. 46, 431–444.
Flores, J.A., Marino, M., 2002. Pleistocene calcareous nannofossil stratigraphy for ODP Leg 177 (Atlantic sector of the Southern Ocean). Mar. Micropaleontol. 45, 191–224.
Flores, J.A., Sierro, F.J., 2007. Pronounced mid-Pleistocene southward shift of the Polar Front in the Atlantic sector of the Southern Ocean. Deep-Sea Res. II 54 (21–22), 2432–2442.
Flores, J.A., Sierro, F.J., Raffi, I., 1995. Evolution of the calcareous nannofossil assemblage as a response to the paleoceanographic change in the Eastern Equatorial Pacific from 4 to 2 Ma (leg 138, Site 849 and 852). Proc. Ocean Drill. Program, Initial Rep. 138, 163–176.
Flores, J.A., Sierro, F.J., Frances, G., Vazquez, A., Zamarreno, I., 1997. The last 1000.000 years in the western Mediterranean: sea surface water and frontal dynamics as revealed by coccolithophores. Mar. Micropaleontol. 29, 351–366.
Flores, J.A., Gersonde, R., Sierro, F.J., 1999. Pleistocene fluctuations in the Agulhas Current Retroflection based on the calcareous plankton record. Mar. Micropaleontol. 37, 1–22.
Flores, J.-A., Bárcena, M.A., Sierro, F.J., 2000a. Ocean-surface and wind dynamics in the Atlantic Ocean off Northwest Africa during the last 140,000 years. Palaeogeogr. Palaeoclimatol. Palaeoecol. 161, 459–478.
Flores, J.-A., Sierro, F.J., Gersonde, R., Niebler, H.S., 2000b. Southern Ocean Pleistocene calcareous nannofossil events: calibration with the isotope and geomagnetic stratigraphies. Mar. Micropaleontol. 40, 377–402.
Flores, J.-A., Sierro, F.J., Filippelli, G.M., Bárcena, M.Á., Pérez-Folgado, M., Vázquez, A., Utrilla, R., 2005. Surface water dynamics and phytoplankton communities during deposition of cyclic late Messinian sapropel sequences in the western Mediterranean. Mar. Micropaleontol. 56, 50–79.
Froelich, P.N., Malone, P.N., Hodell, D.A., Ciesielski, P.F., Warnke, D.A., Westall, F., Hailwood, E.A., Nobles, D.C., Fenner, J., Mienert, J., Mwenifumbo, C.J., Muller, D.W., 1991. Biogenic opal and carbonate accumulation rates in the subantarctic South Atlantic: the Late Neogene of Meteor Rise Site 704. In: Ciesielski, P.F., Kristoffersen, Y., et al. (Eds.), Proc. ODP, Sci. Res., vol. 114, pp. 515–550. College Station, (TX).
Gard, G., 1989. Variations in coccolith assemblages during the last glacial cycle in the high and mid-latitude Atlantic and Indian Oceans. In: Crux, J.A., van Heck, S.E. (Eds.), Nannofossils and their Applications, Proceedings of the International Nannofossil Association Conference, London, 1987. The British Micropalaeontological Society / Ellis Horwood, Chichester, pp. 108–121.
Gard, G., Backman, J., 1990. Synthesis of Arctic and Sub-Arctic coccolith biochronology and History of North Atlantic drift water influx during the last 500,000 years. In: Bleil, U., Thiede, J. (Eds.), Geological History of the Polar Oceans: Arctic versus Antarctic. Kluwer, pp. 417–436.
Gartner, S., 1977. Calcareous nannofossil biostratigraphy and revised zonation of the Pleistocene. Mar. Micropaleontol. 2, 1–25.
Gartner, S., 1988. Paleoceanography of the Mid-Pleistocene. Mar. Micropaleontol. 13, 23–46.
Gartner, S., Chow, J., Stanton, R.J., 1987. Late Neogene paleoceanography of the eastern Caribbean, the Gulf of Mexico, and the eastern Equatorial Pacific. Mar. Micropaleontol. 12 (3), 255–304.
Gersonde, R., Hodell, D.A., Blum, P., 1999. Leg 177 summary: Southern Ocean paleoceanography. Proc. ODP, Init. Repts., vol. 177, pp. 1–67. College Station, (TX).
Giraudeau, J., 1992. Coccolith paleotemperature and paleosalinity estimates in the Caribbean Sea for the Middle-Late Pleistocene (DSDP Leg 68 Hole 502B). Mem. Sci. Geol. 43, 375–387 Padova.
Giraudeau, J., Bailey, G.W., Pujol, C., 2000. A high-resolution time-series analyses of particle fluxes in the Northern Benguela coastal upwelling system: carbonate record of changes in biogenic production and particle transfer processes. Deep-Sea Res. II 47, 1999–2028.
Gordon, A.L., 1996. Comment on the South Atlantic's role in the global circulation. In: Wefer, G., Berger, W.H., Siedler, G., Webb, D. (Eds.), The South Atlantic: Present and Past Circulation. Springer, Berlin, pp. 121–124.
Gordon, A.L., Weiss, R.F., Smethie Jr., W.M., Warner, M.J., 1992. Thermocline and intermediate water communication between the South Atlantic and Indian oceans. J. Geophys. Res. 9 (C5), 7223–7240.
Haidar, A.T., Thierstein, H.R., 1997. Calcareous phytoplankton dynamics at Bermuda (N. Atlantic) EUG 9 Abstr. Terra Nova 9 (Suppl. 1), 602.
Hiramatsu, C., De Deckker, P., 1997. The late Quaternary calcareous nanoplankton assemblages from three cores from the Tasman Sea. Palaeogeogr. Palaeoclim. Palaeoecol. 131, 391–412.
Jordan, R.W., Zhao, M., Eglinnton, G., Weaver, P.P.E., 1996. Coccolith and alkenone stratigraphy and paleoceanography at an upwelling site off NW Africa (ODP 658C) during the last 130,000 years. In: Moguilevsky, A., Whatley, R. (Eds.), Microfossils and Oceanic Environments. Aberystwyth Press, University of Wales, pp. 111–130.
Kuhn, G., Diekmann, B., 2002. Late Quaternary variability of ocean circulation in the southeastern South Atlantic inferred from the terrigenous sediment record of a drift deposit in the southern Cape Basin (ODP Site 1089). Palaeogeogr. Palaeoclimatol. Palaeoecol. 182, 287–303.
Laskar, J., Robutel, P., Joutel, F., Gastineau, M., Correia, A.C.M., Levrard, B., 2004. A long-term numerical solution for the insolation quantities of the Earth. Astron. Astrophys. 428, 261–285. doi:10.1051/0004-6361:20041335.
Lutjeharms, J.R.E., 1981. Features of the southern Agulhas Current circulation from satellite remote sensing. S. Afr. J. Sci. 77, 231–236.
Lutjeharms, J.R.E., 1996. The exchange of water between the South Indian and the South Atlantic. In: Wefer, G., Berger, W.H., Siedler, G., Webb, D. (Eds.), The South Atlantic: Present and Past Circulation. Springer, Berlin, pp. 125–162.
Lutjeharms, J.R.E., van Ballegooyen, R.C., 1984. Topographic control in the Agulhas Current system. Deep-Sea Res. 31 (11), 1321–1337.
Lutjeharms, J.R.E., Valentine, H.R., 1984. Southern Ocean thermal fronts south of Africa. Deep-Sea Res. 31, 1461–1476.
Maiorano, P., Marino, M., 2004. Calcareous nannofossil bioevents and environmental control on temporal and spatial patterns at the early-middle Pleistocene. Mar. Micropaleontol. 53, 405–422.
Matsuoka, H., Okada, H., 1989. Quantitative analysis of Pleistocene nannoplankton in the subtropical northwestern Pacific Ocean. Mar. Micropaleontol. 14, 97–118.
McIntyre, A., Bé, A.H.W., 1967. Modern coccolithophores of the Atlantic Ocean — I. Placolith and cyrtoliths. Deep-Sea Res. 14, 561–597.
McIntyre, A., Ruddiman, W.F., Jantzen, R., 1972. Southward penetrations of the North Atlantic Polar Front: faunal and floral evidence of large-scale surface water mass movements over the last 225,000 years. Deep-Sea Res. 19, 61–77.

Molfino, B., McIntyre, A., 1990. Nutricline variation in the equatorial Atlantic coincident with the Younger Dryas. Paleoceanography 5, 997–1008.

Narciso, A., Cachão, M., de Abreu, L., 2006. *Coccolithus pelagicus* subsp. *pelagicus* versus *Coccolithus pelagicus* subsp. *braarudii* (Coccolithophore, Haptophyta): a proxy for surface subartic Atlantic waters off Iberia during the last 200 kyr. Mar. Micropaleontol. 59, 15–34.

Okada, H., Honjo, S., 1973. The distribution of oceanic coccolithophorids in the Pacific. Deep-Sea Res. 20, 355–374.

Okada, H., Wells, P., 1997. Late Quaternary nannofossil indicators of climate change in two deep-sea cores associated with the Leeuwin Current off Western Australia. Paleogeogr. Paleoclim. Paleoecol. 131, 413–432.

Ou, H.W., de Ruijter, W.P.M., 1986. Separation of an inertial boundary current from a curved coastline. J. Phys. Oceanogr. 16, 280–289.

Parente, A., Cachão, M., Baumann, K.-H., de Abreu, L., Ferreira, J., 2004. Morphometry of *Coccolithus pelagicus* s.l. (Coccolithophore, Haptophyta) from offshore Portugal, during the last 200 kyr. Micropaleontology 50, 107–120.

Peeters, F.J.C., Acheson, R., Brummer, G.-J.A., de Ruijter, W.P.M., Ganssen, G.M., Schneider, R.R., Ufkes, E., Kroon, D., 2004. Vigorous exchange between Indian and Atlantic Ocean at the end of the last five glacial periods. Nature 430, 661–665.

Pether, J., 1994. Molluscan evidence for enhanced deglacial advection of Agulhas water in the Benguela Current, off southwest Africa. Palaeogeogr. Palaeoclimatol. Palaeoecol. 111, 99–117.

Petschick, R., Kuhn, G., Gingele, F.X., 1996. Clay mineral distribution in surface sediments of the South Atlantic: sources, transport, and relation to oceanography. Mar. Geol. 130, 203–229.

Pujos, A., 1992. Ca1careous nannofossils and the <25 µm fraction in Quaternary sediments of the subtropical NE Atlantic Oceano. Proc. INA Florence Meet. Mem. Sci. Geol., vol. 43, pp. 409–429. Padova.

Raffi, I., 2002. Revision of the early-middle Pleistocene calcareous nannofossil biochronology (1.75–0.85 Ma). Mar. Micropaleontol. 45, 25–55.

Raffi, I., Backman, J., Rio, D., Shackleton, N.J., 1993. Early Pleistocene and late Pliocene nannofossil biostratigraphy and calibration to oxygen isotope stratigraphies from DSDP Site 607 and ODP Site 677. Paleoceanography 8, 387–404.

Raffi, I., Backman, J., Fornaciari, E., Pälike, H., Rio, D., Lourens, L., Hilgen, F., 2006. A review of calcareous nannofossil astrobiochronology encompassing the past 25 million years. Quat. Sci. Rev. 25, 3113–3137.

Reason, C.J.C., 2001. Evidence for the influence of the Agulhas Current on regional atmospheric circulation patterns. J. Climate 14, 2769–2778.

Renaud, S., Ziveri, P., Broerse, A.T.C., 2002. Geographical and seasonal differences in morphology and dynamics of the coccolithophore *Calcidiscus leptoporus*. Mar. Micropaleontol. 46, 363–385.

Rio, D., Raffi, I., Villa, G., 1990. Pliocene–Pleistocene calcareous nannofossil distribution patterns in the western Mediterranean. In: Kastens, K.A., Mascle, J., et al. (Eds.), Proc. ODP, Sci. Res., vol. 107, pp. 513–533. College Station (TX).

Roth, P.H., 1994. Distribution of coccoliths in oceanic sediments. In: Winter, A., Siesser, W. (Eds.), Coccolithophores. Cambridge University Press, Cambridge, pp. 199–218.

Roth, P.H., Coulbourn, W.T., 1982. Floral and solution patterns of coccoliths in surface sediments of the North Pacific. Mar. Micropaleontol. 7, 1–52.

Scherer, R., Bohaty, S.M., Harwood, D., Roberts, A., Taviani, M., 2003. Marine Isotope Stage 31 (1.07 Ma): an extreme interglacial in the Antarctic nearshore zone. Geophys. Res. Abstr. 5, 11710 2003 European Geophysical Society 2003.

Scherer, R.P., Bohaty, S.M., Dunbar, R.B., Esper, O., Flores, J.-A., Gersonde, R., Harwood, D.M., Roberts, A.P., Taviani, M., 2008. Antarctic records of precession-paced insolation-driven warming during early Pleistocene Marine Isotope Stage 31. Geophys. Res. Lett. 35, L03505. doi:10.1029/2007GL032254.

Schouten, M.W., de Ruijter, W.P.M., van Leeuwen, P.J., Dijkstra, H.A., 2002. An oceanic teleconnection between the equatorial and southern Indian Ocean. Geophys. Res. Lett. 29 (16) doi:101029/2001GL014542 (2002).

Takahashi, K., Okada, H., 2000. Environmental control on the biogeography of modern coccolithophores in the southeastern Indian Ocean offshore of Western Australia. Mar. Micropaleontol. 39, 73–86.

Teitler, L., Kupp, G., Warnke, D., Burckle, L., 2007. Evidence for a long warm interglacial during Marine Isotope Stage 31: comparison of two studies at proximal and distal marine sites in the Southern Ocean. U.S. Geological Survey and The National Academies; USGS OF-2007-1047, Extended Abstract 013.

Venz, K., Hodell, D.A., 2002. New evidence for changes in Plio-Pleistocene deep water circulation from Southern Ocean ODP Leg 177 Site 1090. Palaeogeogr. Palaeoclimatol. Palaeoecol. 182, 197–220.

Villa, G., Lupi, C., Cobianchi, M., Florindo, F., Pekar, S.F., 2008. A Pleistocene warming event at 1 Ma in Prydz Bay, East Antarctica: evidence from ODP Site 1165. Palaeogeogr. Palaeoclimatol. Palaeoecol. 260, 230–244.

Weaver, P.P.E., Pujol, C., 1988. History of the last deglaciation in the Alboran Sea (western Mediterranean) and adjacent North Atlantic as revealed by coccolith floras. Paleogeogr. Paleoclim. Paleoecol. 64, 35–42.

Wei, W., 1993. Calibration of upper Pliocene–lower Pleistocene nannofossil events with oxygen isotope stratigraphy. Paleoceanography 8, 85–89.

Wells, P., Okada, H., 1997. Response of nannoplankton to major changes in sea-surface temperature and movements of hydrological fronts over Site DSDP 594 (south Chatham Rise, southeastern New Zealand), during the last 130 kyr. Mar. Micropaleontol. 32, 341–363.

Westall, F., Fenner, J., 1991. Pliocene–Holocene Polar Front Zone in the South Atlantic: changes in its position and sediment-accumulation rates from Holes 699A, 701C, and 704B. In: Ciesielski, P.F., Kristoffersen, Y., et al. (Eds.), Proc. ODP, Sci. Res., vol. 114, pp. 609–646. College Station, (TX).

Ziveri, P., Thunell, R.C., Rio, D., 1995. Export production of coccolithophores in an upwelling region: results from San Pedro Basin, Southern California Borderlands. Mar. Micropaleontol. 24, 335–358.

Ziveri, P., Rutten, A., de Lange, G.J., Thomson, J., Corselli, C., 2000. Present-day coccolith fluxes recorded in central eastern Mediterranean sediment traps and surface sediments. Paleogeogr. Paleoclimatol. Paleoecol. 158, 175–195.

Ziveri, P., Baumann, K.-H., Boeckel, B., Bollmann, J., Young, J., 2004. Biogeography of selected Holocene coccoliths in the Atlantic Ocean. In: Thierstein, H.R., Young, Y.R. (Eds.), Coccolithophores from Molecular Processes to Global Impact. Springer, Berlin, pp. 403–428.